

“Killer” Microcapsules That Can Selectively Destroy Target Microparticles in Their Vicinity

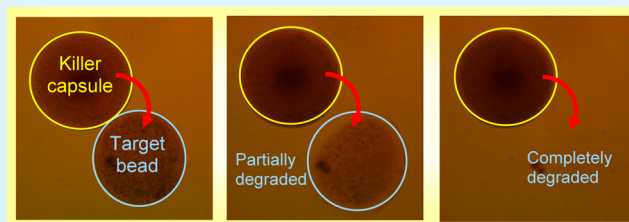
Chandamany Arya, Hyuntaek Oh, and Srinivasa R. Raghavan*

Department of Chemical & Biomolecular Engineering, University of Maryland, College Park, Maryland 20742, United States

S Supporting Information

ABSTRACT: We have developed microscale polymer capsules that are able to chemically degrade a certain type of polymeric microbead in their immediate vicinity. The inspiration here is from the body’s immune system, where killer T cells selectively destroy cancerous cells or cells infected by pathogens while leaving healthy cells alone. The “killer” capsules are made from the cationic biopolymer chitosan by a combination of ionic cross-linking (using multivalent tripolyphosphate anions) and subsequent covalent cross-linking (using glutaraldehyde). During capsule formation, the enzyme glucose oxidase (GOx) is encapsulated in these capsules. The target beads are made by ionic cross-linking of the biopolymer alginate using copper (Cu^{2+}) cations. The killer capsules harvest glucose from their surroundings, which is then enzymatically converted by GOx into gluconate ions. These ions are known for their ability to chelate Cu^{2+} cations. Thus, when a killer capsule is next to a target alginate bead, the gluconate ions diffuse into the bead and extract the Cu^{2+} cross-links, causing the disintegration of the target bead. Such destruction is visualized in real-time using optical microscopy. The destruction is specific, i.e., other microparticles that do not contain Cu^{2+} are left undisturbed. Moreover, the destruction is localized, i.e., the targets destroyed in the short term are the ones right next to the killer beads. The time scale for destruction depends on the concentration of encapsulated enzyme in the capsules.

KEYWORDS: biodegradable capsules, biomimetic materials, bioinspired systems, microfluidic synthesis, polysaccharides



INTRODUCTION

Microcapsules having a liquid core and a solid shell are widely used in consumer products, nutraceuticals, agrochemicals, and biomedical applications.^{1–3} These structures can encapsulate a variety of different payloads in their core, including drugs, cosmetics, or flavor molecules. The payload in the microcapsules can be released steadily over a long time or can be released in a burst at a specific time or in response to a stimulus such as temperature or light.^{4,5} Microcapsules have also attracted recent attention in a very different context, which is in the design of “artificial cells” or protocells.^{6,7} The motivation in this context is to construct simple container structures using either synthetic polymers, biopolymers, or lipids that can mimic some basic functions of a biological cell. For example, Bentley et al.⁸ have developed biopolymer capsules having the ability to communicate with bacterial populations through small signaling molecules.

The inspiration for this work comes from the cells in the body’s immune system.^{9,10} The function of the immune system is to protect the body against invaders such as viruses and bacteria. If these pathogens are somehow able to enter the body and infect some cells, the immune system quickly tries to identify and eliminate the infected cells, so that the damage is minimized. For this purpose, one of the main types of immune cells are the cytotoxic T lymphocytes (CTLs), also called “killer” T cells (Figure 1a).^{10–12} These cells contain the machinery for targeted destruction of infected cells. For

example, the cells can generate and secrete cytotoxic proteins such as perforin and granzymes. The killer T cells move close to the infected cells and locally secrete the cytotoxic proteins, packaged within nanoscale containers called exosomes (Figure 1a).^{11,12} The proteins enter the infected cells and induce cell death (apoptosis), thereby ensuring that the pathogens in them are not propagated further. Because protein release is confined to the infected cells, normal (uninfected) neighboring cells are left alone (Figure 1a). The same killer T cell can then move on and use the same mechanism to eliminate other infected cells.

In this paper, we report the development of microparticles that are inspired by the killer T cells (Figure 1b). As noted above, these cells have the ability to selectively destroy infected cells while sparing normal ones. This property is translated into an abiotic system involving different kinds of polymeric microparticles. Specifically, we develop a class of “killer” microcapsules made from the biopolymer chitosan, with the enzyme glucose oxidase (GOx) encapsulated in them. In the presence of glucose from the external environment, these killer capsules continuously generate gluconate ions, which are a known chelator of metal ions such as copper (Cu^{2+}). Thus, the killer capsules can selectively attack particles that are cross-linked by metal ions. Here, the targets are microbeads formed

Received: August 11, 2016

Accepted: October 3, 2016

Published: October 19, 2016

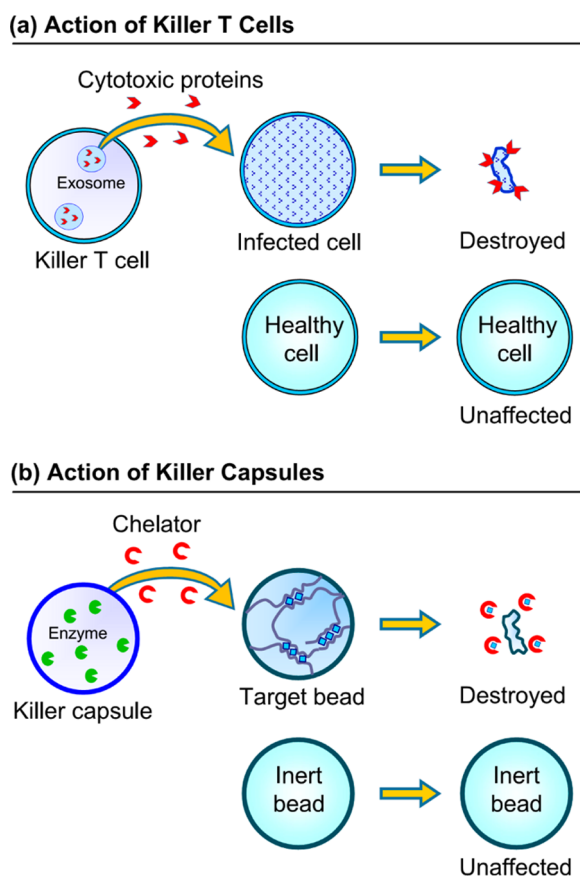


Figure 1. Analogy between killer T cells of the immune system and “killer” capsules. (a) The killer T cells target cells in the body that are infected by pathogens or cancer. Cytotoxic proteins packaged in exosomes are dispatched out, whereupon they enter the infected cell and induce cell death. Healthy cells are left undisturbed. (b) The “killer” capsules in this study generate chelator molecules, which diffuse into target beads in their vicinity. The chelator removes metal cross-links from the beads, thereby destroying them. Inert beads that do not have these metal cross-links remain unaffected.

by cross-linking the biopolymer alginate with Cu^{2+} ions. When the killer capsules and target beads are mixed, the gluconate released from the capsules removes the Cu^{2+} from alginate beads in the vicinity of the capsules, causing the destruction of the beads (Figure 1b). Other microparticles that are not cross-linked by metal ions are unaffected, i.e., they remain as inert bystanders (Figure 1b). The destructive effect is localized near the killer capsules (in the short term) because it relies on diffusion of the chelating gluconate molecules from the capsules to the target beads. This is analogous to the diffusion of cytotoxic proteins from the killer T cells to infected cells.^{11,12} Overall, this is the first study, to the best of our knowledge, to explore the idea of using one polymer particle as the vehicle to destroy another specific particle. The concept here could be useful in the development of protocells, drug-delivery vehicles, or tissue-engineering constructs with even more sophisticated functionalities.

RESULTS AND DISCUSSION

Figure 2 shows the microfluidic setup used in this study for forming microcapsules and microbeads. This setup was developed in our lab previously and has been described in more detail elsewhere.^{13,14} It allows for the generation of

microscale aqueous droplets at the tip of a capillary. A key distinguishing feature of this method over other microfluidic methods is that we do not use an immiscible oil phase to form the aqueous droplets.^{15,16} Instead, pulses of compressed air or nitrogen gas are used to shear off the droplets from the capillary tip. To generate these pulses, we connect a gas-flow controller to a function generator. The gas flows as a sheath around the tip of an inner glass capillary of diameter of $\sim 100 \mu\text{m}$ in which an aqueous solution is flowed (the liquid flow is controlled by a syringe pump). For every pulse of gas, an aqueous droplet is dislodged from the tip of the inner capillary. The flow rate of the liquid as well as the frequency of the pulsing gas dictate the volume of the liquid droplet. Droplets generated by this technique are very uniform, with polydispersities of $<3\%$ in their diameter.¹³

Our approach to forming capsules and beads utilizes particular biopolymers in the generating solution that passes through the inner capillary and cross-linker(s) for these biopolymers in the reservoir solution where the droplets are collected. To form the “killer” capsules, we use the cationic biopolymer chitosan in the generating solution.^{17–20} Together with 2 wt % chitosan, this solution also contains the enzyme GOx at a concentration of 200 units/mL. In the reservoir, we use a 10 wt % solution of sodium tripolyphosphate (TPP). TPP is a multivalent anion that is known to cross-link chitosan by forming ionic interactions with multiple chitosan chains.²¹ We create droplets of chitosan–GOx, which are dropped into the TPP solution and allowed to incubate for 30 min. In this time, the droplets are converted into soft capsules due to TPP cross-linking.^{21–23} Thereafter, the solution in the reservoir is replaced with a solution of 1 wt % glutaraldehyde (GA), which is a dialdehyde that reacts with the amines on chitosan, forming covalent cross-links.^{20,23} GA strengthens the chitosan–TPP capsules. The capsules are then washed and stored in deionized (DI) water. On the basis of previous studies, it is known that the shell of these capsules is porous to small molecules but not to nanoscale structures or macromolecules such as the GOx enzyme (molecular weight $\sim 160 \text{ kDa}$).^{8,19,24} Thus, GOx is entrapped within the lumen of the killer capsules.

Next, to prepare the target beads, we use a 2 wt % solution of the anionic biopolymer sodium alginate as the generating solution and 1 wt % of copper sulfate (CuSO_4) in the reservoir solution. In the process, droplets of sodium alginate are cross-linked by Cu^{2+} cations to form the target beads.²⁵ Consistent with the literature, we refer to these alginate particles as beads rather than capsules because they are expected to be uniformly cross-linked rather than having a core–shell structure.^{25–27} The diameters of both the killer capsules and the target beads are $\sim 300 \mu\text{m}$ in our study. Note that their sizes are determined by the sizes of the droplets, which can be varied easily between ~ 50 to $500 \mu\text{m}$. A few studies are also conducted with larger (millimeter scale) capsules and beads, and in this case, instead of the above capillary-based setup, a 22 gauge syringe is used to directly inject droplets of the respective biopolymer solutions into the collecting reservoir.

Figure 3 (top) shows the mechanism by which the killer capsules (bearing GOx) are expected to attack their target Cu–alginate beads. For this, the external medium must contain glucose, which is the substrate for GOx.^{22,28} We expect glucose to diffuse from the surroundings into the killer capsule (step A). The enzymatic catalysis of glucose by GOx (in the presence of oxygen) will first result in the intermediate D-glucono- δ -lactone (GDL), which will then be hydrolyzed to form

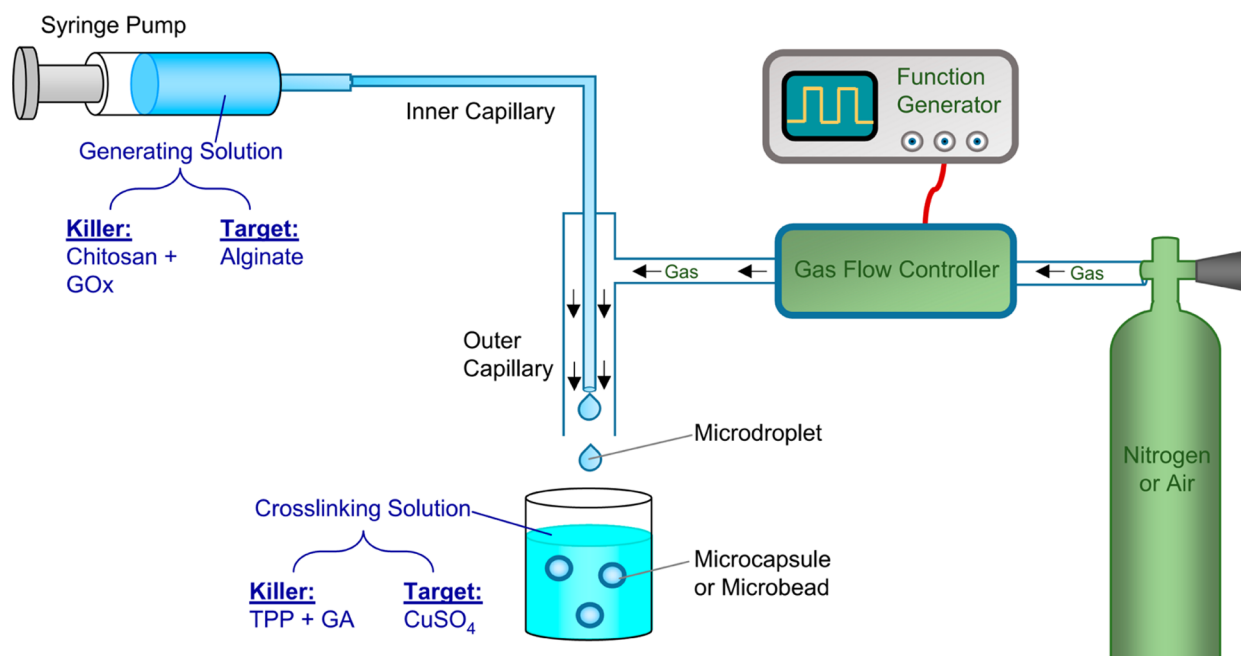


Figure 2. Synthesis of microcapsules and microbeads by an oil-free microfluidic technique. Microdroplets bearing a biopolymer of interest are generated by flowing the aqueous biopolymer solution through an inner capillary. Gas (nitrogen or air) is flowed through an outer capillary that sheaths the inner one. The gas is flowed in pulses, which are controlled by the function generator. The result is that uniform aqueous droplets emerge from the tip of the inner capillary. These droplets are introduced into an appropriate cross-linking solution (also aqueous). For the killer capsules, the generating solution is composed of chitosan, along with the enzyme GOx. The cross-linking solution contains the anion TPP, and the dialdehyde GA is introduced thereafter. For the target beads, the generating solution is composed of alginate, and the cross-linking solution is based on divalent Cu²⁺ cations.

gluconate ions (step B).²⁸ These ions will then diffuse out of the capsule into the external solution, and if a target Cu–alginate bead is present nearby, the gluconate ions will diffuse into the bead (step C). At that point, the gluconate will chelate the Cu²⁺ cations that form the cross-links in the bead.^{29,30} Thereby, the target bead will be degraded into soluble alginate chains (step D). Incidentally, the equilibrium constant for chelation of Cu²⁺ by gluconate is 2×10^{18} , whereas for chelation by gluconate of Ca²⁺ and Sr²⁺ (two other divalent cations commonly used to cross-link alginate), the equilibrium constants are much lower (~ 10).³⁰ In other words, gluconate is much more efficient at chelating Cu²⁺, which is why we used Cu²⁺ as the cross-linking cation for our target alginate beads rather than Ca²⁺ or Sr²⁺.

To test the above concept, we combined our killer capsules and target beads in an HEPES buffer solution (pH 7.4) containing 1 wt % glucose. Then, we observed the system using optical microscopy. In the bottom portion of Figure 3, the focus is on a pair of such particles and representative images of this pair are shown at selected time points. (The entire process is also shown in Movie 1.) Consistent with the expected mechanism, the images clearly demonstrate degradation of the target bead as time progresses. The degradation begins at the side of the bead that is closest to the killer capsule (Images 2 and 3). Over time, the degradation proceeds inward (i.e., toward the core). At the 4 h mark (Image 5), more than half of the bead has been degraded, and the portion that remains is barely visible. Note that the degradation is expected to result in uncross-linked alginate chains (Panel D), which can diffuse away from the original location of the target bead. By the 5 h mark (Image 6), the degradation appears to be complete and no portion of the bead is visible any more. Note that the above

experiments were conducted in HEPES buffer, a common buffer that does not interact with metal ions.³¹ The buffer is needed to maintain pH because with a lowering of pH by more than one unit, the chelation efficiency of gluconate drops,³⁰ and moreover, alginate beads tend to shrink.^{25–27}

The degradation seen in Figure 3 is quantified in Figure 4. For this, images at regular time points were analyzed, and the size of the target bead (area on the image) was calculated in each case. The size (as a percent relative to its initial value) as a function of time is plotted in Figure 4a. The striking result is that there is a 20% increase in bead size initially (up to ~ 200 min) before the size decreases. This can be explained as follows. As the gluconate diffuses into the bead, it removes Cu²⁺ cross-links, which causes the bead to swell more in water.^{26,27} Indeed, one can see from the initial images that the bead appears less opaque as it is getting degraded, which is evidently because more water has entered into it. After the 200 min mark, most of the cross-links have been removed from the outer regions of the bead, and from this point onward, there is a visible reduction in size. The same trend as in Figure 4a is seen for every target bead analyzed. Our findings imply that, to accurately measure the degradation of the bead from the images, one must account for two factors: the decrease in area as well as in opacity, as explained further in Figure S1. Using this approach, we show in Figure 4b a plot of the undegraded (i.e., remaining) fraction of the bead versus time corresponding to the data in Figure 4a. This plot shows a monotonic decrease with time until the value falls to zero (i.e., 100% degradation) at the 300 min mark. Over the first 100 min, there is negligible degradation on the whole. This is because some time is required for gluconate to build up by enzymatic reaction and

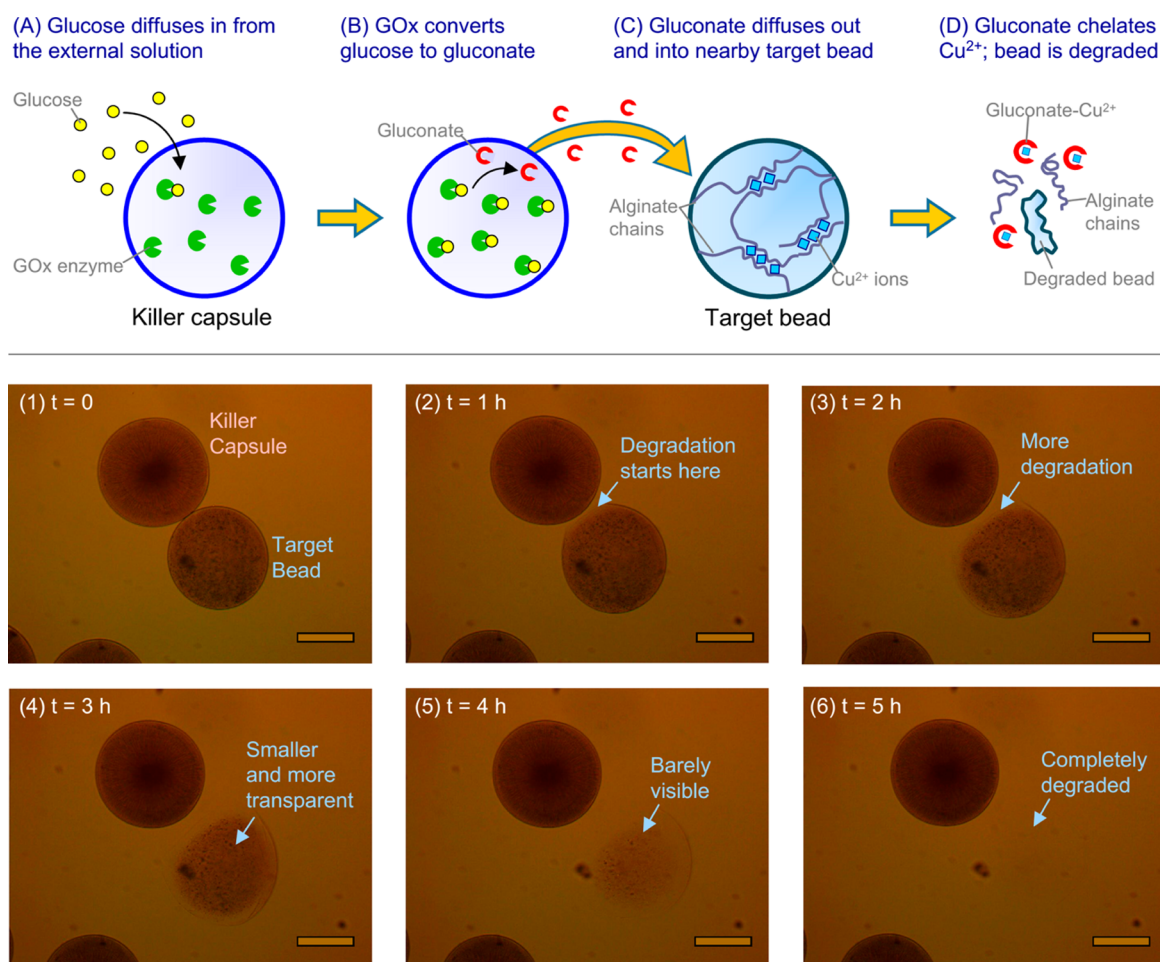


Figure 3. Mechanism by which a killer capsule destroys a target bead (top) and images depicting this process over time (bottom). Top: The killer capsule contains the enzyme GOx. Glucose from the surroundings diffuses into the capsule (step A), forming gluconate (step B), which diffuses out and into nearby target beads (step C). The target bead is formed by cross-linking alginate with Cu^{2+} cations. The gluconate chelates away the Cu^{2+} , and thereby the bead is degraded, leaving behind uncross-linked alginate chains (step D). Bottom: Images from optical microscopy of a killer capsule next to a target bead in a quiescent solution containing 1 wt % glucose. As time progresses, the gluconate diffuses into the bead and causes degradation. The degradation begins on the side of the bead that is closest to the capsule (Images 2 and 3). As the bead continues to degrade, its size reduces, and it becomes more transparent (Images 4 and 5). After 5 h (Image 6), the degradation is complete, and the bead cannot be seen any more. The above process is also shown from start to finish in [Movie 1](#). Scale bars in the images are 150 μm .

then diffuse into the bead. Once sufficient gluconate has entered the bead, degradation proceeds more rapidly.

To prove that the degradation of the target bead is indeed due to (a) the enzymatic action of GOx on glucose and, in turn, (b) the chelation of Cu^{2+} by the reaction product, gluconate, we performed a series of additional experiments. Macroscale (millimeter-sized) killer and target beads were used for these experiments, and the results are shown in [Figures S2 and S3](#). First, we confirmed that target (Cu–alginate) beads can be degraded by exposure to free GOx in the external solution. For this experiment, the beads were placed in a solution containing 1 wt % glucose and 1 unit/mL of GOx. The representative images in [Figure S2](#) show that the beads degrade over the course of 6 h. As controls, the same experiment with Cu–alginate beads was repeated in a solution of GOx enzyme (no glucose) and in a solution of glucose (no enzyme). No degradation was observed (even over several days) for these control cases. Thus, degradation of the beads requires both the enzyme and the substrate to be present, which confirms that it is the result of the enzymatic reaction, i.e., due to the gluconate (Cu^{2+} chelator) being formed.

Next, we confirmed that macroscale killer capsules can degrade corresponding target beads ([Figure S3](#)). Because these structures are larger, they can be observed visually (both have diameters of ~ 2.5 mm). The killer chitosan capsule in [Figure S3](#) is loaded with an orange dye, and the target Cu–alginate bead has a blue-green dye. Their compositions are otherwise identical to those in [Figure 3b](#), i.e., the killer has 200 units/mL of GOx inside, the external solution is HEPES buffer with 1 wt % glucose, and the target is cross-linked using 1 wt % CuSO_4 . [Figure S3](#) confirms that the Cu–alginate bead gets degraded over a period of 18 h. The time scale is longer than for the corresponding microscale particles, which is because degradation is controlled by the diffusion of gluconate from the killer to target bead. The diffusion time scale is expected to vary as $\tau \approx a^2/\mathcal{D}$, where a is distance and \mathcal{D} is the diffusivity.³² The total distance that the gluconate has to diffuse is composed of two parts: (i) the distance from the killer to the target; and (ii) the sizes of the killer and the target. In the macroscale experiment, the killer and target are positioned a few mm from each other, and they are too large to diffuse away. Thus, the gluconate will take quite some time to reach the exterior of the target bead

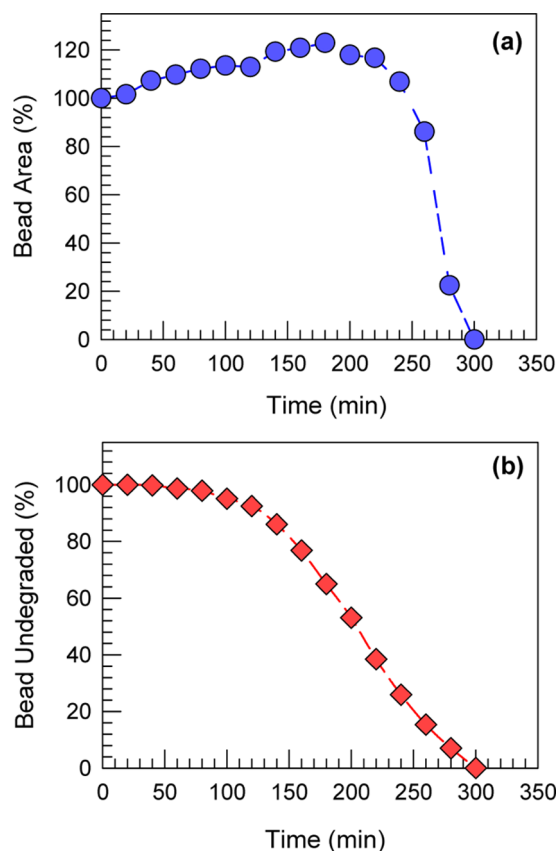


Figure 4. Kinetics of target bead degradation due to the action of the killer capsule. The images in Figure 3 are analyzed to obtain the data shown in these plots. (a) Change in bead area, relative to its initial size, vs time. The area increases initially and then decreases to zero. (b) Percent of bead that is left undegraded, as calculated by accounting for both the bead area and its opacity. This quantity decreases monotonically with time and falls to zero in ~ 300 min.

and furthermore to diffuse all the way across the target. Using the above setup, we also studied the effect of enzyme concentration, with all other parameters kept constant. Instead of 200 units/mL of GOx in the killer capsule, we examined enzyme levels that were lower or higher by an order of magnitude. Figure S4 shows that the degradation time decreases monotonically with increasing enzyme concentration, as expected.²⁴

Targeted bead degradation in the above manner could enable the localized release of trapped cargo from the beads. To demonstrate this, we encapsulated fluorescent nanoparticles (diameter ~ 100 nm) at a concentration of 0.2 wt % within a target Cu–alginate macrobead. A killer chitosan capsule was then placed next to this target bead, and the two were studied in a buffered 1 wt % glucose solution (both the capsule and bead have diameters of ~ 2.5 mm). Images of the pair using both bright-field and fluorescence microscopy are shown in Figure S5. Initially, the fluorescent nanoparticles are encapsulated within the target bead, and so the fluorescence is confined within the bead volume. As the Cu^{2+} cross-links are removed from the target bead, the nanoparticles get released into the surrounding solution (they are small enough to diffuse rapidly). As a result, we see the emergence of background fluorescence in the solution once the bead is sufficiently degraded.²⁴

Finally, we conducted an experiment to demonstrate the specificity in destruction of target microbeads by the killer

capsules. In the immune system, killer T cells destroy infected cells, whereas they leave healthy cells alone (Figure 1a). Our abiotic system is also specific, and to show this, we synthesized three different populations of microparticles and mixed them in roughly equal numbers in a solution of 1 wt % glucose (Figure 5). The first population is of killer chitosan capsules with a diameter of ~ 300 μm and with 200 units/mL of GOx inside. Another population is of Cu–alginate target beads with a diameter of ~ 300 μm as well. Both the killer and the target particles are identical to those in Figure 3. Additionally, we synthesized a third population to represent inert particles. These were made by the same microfluidic procedure as in Figure 2, but for the generating solution, an aqueous solution of 2 wt % chitosan with 1 wt % of carbon black (CB) particles dispersed in it was used, and for the reservoir solution, 2 wt % of GA was used. Also, the droplets were incubated in the GA solution for a full day, thus resulting in uniformly cross-linked chitosan–GA beads.²⁰ Moreover, the flow rates were adjusted such that the diameters of these inert beads was ~ 150 μm , i.e., about half the sizes of the killer and target. To distinguish the three sets of particles in Figure 5, we have marked the killers with yellow circles and the targets with blue circles. Note that the killers can be distinguished also by the presence of a darker central core in each of them, which is not present in the targets. The inerts have a uniform black color due to the encapsulated CB, and they are also smaller than the rest of the particles.

Figure 5 depicts the changes in the above system as a function of time. Because the system is quiescent, i.e., there is no convective mixing, the particles remain in roughly the same position over the period of observation. The changes in the system are caused by the generation of gluconate in the killer capsules and the subsequent diffusion of these molecules throughout the sample. As expected, the gluconate degrades the Cu–alginate target beads (by chelating the Cu^{2+}), but the inert beads (that do not contain any Cu^{2+}) are left undisturbed. At the intermediate time point of 4 h (Figure 5b), we note that several target beads have been eliminated, i.e., there are fewer blue particles compared to those at $t = 0$. Moreover, as can be seen by the zoomed image in Figure 5b, the surviving target beads are more transparent compared to their initial state, indicating partial degradation. Subsequently, by the 8 h mark (Figure 5c), degradation of the target beads is complete, i.e., there are no blue particles left in this image. However, all of the inert beads remain in this case. This confirms the selective nature of the degradation.

The degradation profiles of individual beads in Figure 5 show interesting differences. Specifically, because degradation relies on diffusion of chelator from the killer capsules, it varies based on the location of the target bead relative to the killers. Two cases are analyzed in Figure 6 to highlight this point. First, we focus on a target bead labeled “Close”, i.e., it has four killer capsules that are close to it. The shortest distance between the four killers to this bead is indicated using yellow lines in Image 1 of Figure 6. The proximity to several killers ensures that the bead will be rapidly exposed to chelator molecules. We have analyzed the degradation of the bead from the images, accounting for both its decrease in area as well as opacity, as was done in Figure 4b. The plot of undegraded (i.e., remaining) fraction of the bead versus time shows a steady drop from the outset, and the degradation of the bead is complete in ~ 250 min (thus, this bead is no longer observable at the 4 h mark in Figure 5b). In contrast, we consider a “Distant” target bead, which has four killers that are relatively far away, as indicated by

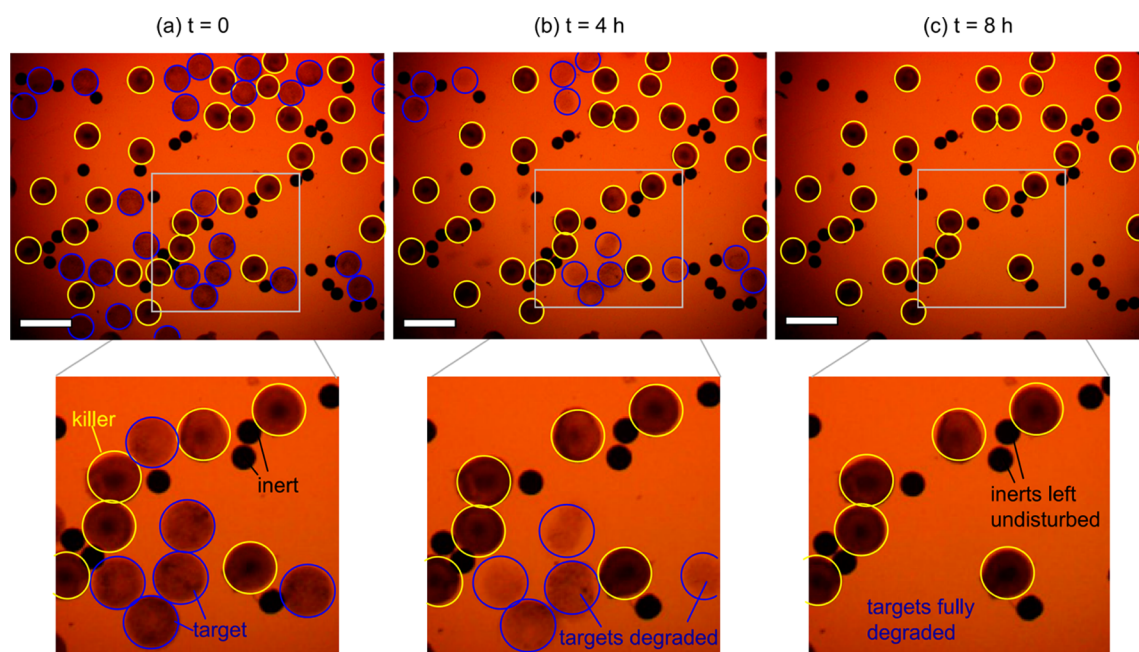


Figure 5. Demonstration that killer capsules degrade target beads but do not affect inert beads. A total of three types of microparticles are combined in a 1 wt % glucose solution, and representative images of the quiescent system are shown over time. For clarity, the killer capsules (chitosan–GOx) are circled yellow, and the target beads (alginate–Cu²⁺) are circled blue. The inert beads (chitosan–GA with carbon black) are not circled and are smaller (150 μm in diameter) than the other two, which are each 300 μm in diameter. (a) At $t = 0$, all three types of particles are observed in the image, as also shown by a zoomed view at the bottom. (b) After 4 h, several of the target beads have been completely degraded and are no longer visible. Other target beads are partially degraded and appear more transparent than at the outset. (c) After 8 h, all of the target beads are completely degraded and are no longer visible in the image, while all of the inert beads remain undisturbed. Scale bars in the images are 600 μm .

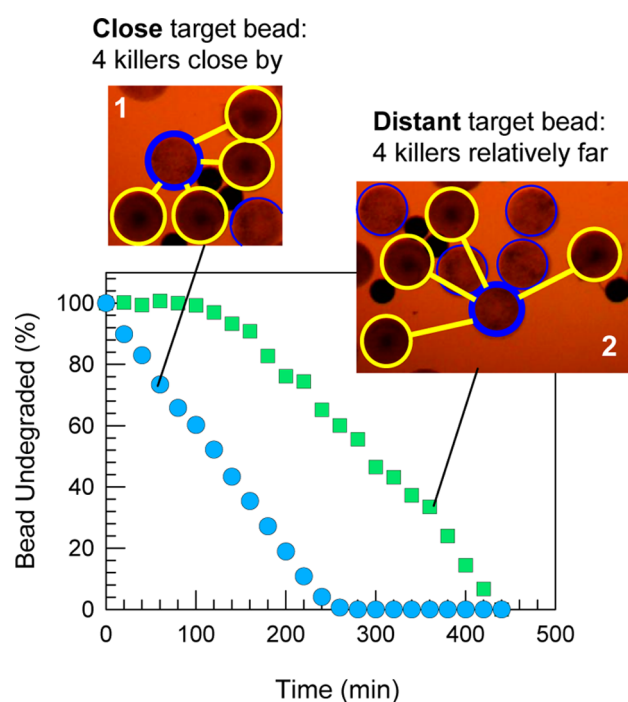


Figure 6. Kinetics of target bead degradation is shown to depend on proximity to killer capsules. The images in Figure 5 are analyzed, and two specific cases are contrasted. The “Close” target bead has four killer capsules close by, as shown by the yellow lines in Image 1. A plot of percent undegraded vs time shows that the degradation of this bead begins at $t = 0$ and is completed by ~ 250 min. In contrast, the “Distant” target bead is relatively far from four killer capsules, as shown by the lines in Image 2. In this case, degradation begins after a lag time of ~ 150 min and is completed only after ~ 450 min.

the longer lines in Image 2. In this case, a plot of undegraded fraction versus time shows a lag time of ~ 150 min before degradation starts. Thereafter, the rate of degradation (slope of the plot) is also lower. Thus, complete degradation of this bead is only accomplished in ~ 450 min.

The above results show that the destruction caused by the killers is local, i.e., in the short term, it is localized toward targets that are very close to (one or more) of the killers. In the simplest analysis, the killers are “point sources” of gluconate, and the diffusion of gluconate away from the killers is governed by Fick’s second law.³² Thus, as one proceeds radially away from a given killer, the concentration of gluconate (at any instant of time) decreases exponentially with radial distance. Because the killers are randomly distributed at $t = 0$ (see Figure 5a), there are numerous sources of gluconate and it is difficult to analyze the system quantitatively. At long times, the gluconate concentration everywhere in the sample reaches a steady-state value, and as a result, all target beads are exposed to sufficient gluconate to cause degradation. Thus, given enough time, all the target beads will get degraded, as demonstrated in Figure 5c.

CONCLUSIONS

We have developed killer capsules made from chitosan that contain the enzyme GOx. These capsules are demonstrated to degrade target beads of alginate cross-linked by Cu²⁺ cations. The degradation occurs in a medium containing glucose, which is the substrate for GOx. Glucose diffuses into the capsules, where it is converted to gluconate ions, which in turn diffuse out of the capsules. When these ions encounter the alginate–Cu²⁺ beads, they remove the Cu²⁺ cross-links by chelation due to which the bead is degraded. Cu²⁺ was chosen as the cation for the beads because of its high chelation efficiency with

gluconate. Target beads that are very close to the killer capsules are affected first by the gluconate. Thus, at short time scales, the destructive effect is localized near the killer capsules.

Our study advances the concept of having one particle destroy another. This should be extendable in multiple ways using other chemistries. Glucose is our molecular cue as it is the substrate for our enzymatic reaction. Other enzyme–substrate couples could be similarly employed. Also, while our idea has been to exploit the product of an enzymatic reaction for inducing the degradation, other products of nonenzymatic reactions or self-assembly processes could also be exploited. We should also point that at the heart of our system there lies a “cascade” process. That is, our molecular cue (glucose) does not by itself cause the end effect (“killing”). Instead the cue (A) has an initial effect (B), which here is production of gluconate, and this in turn causes the final effect (C), which is the destruction of the target. Cascade processes frequently occur in biology and are also being studied in the context of cell-like containers. Here, a key point is that the initial effect (B) occurs in one location, i.e., the capsules, whereas the final effect (C) occurs in a different location, i.e., the beads, with the two locations being connected by diffusion.

MATERIALS AND METHODS

Materials and Chemicals. The following chemicals were obtained from Sigma-Aldrich: the biopolymers, chitosan (medium molecular weight; degree of deacetylation: ~80%) and sodium alginate (low viscosity, molecular weight: 110–150 kDa); the enzyme GOx (from *Aspergillus niger*, 100 000 units/g); and the chemicals sodium tripolyphosphate (TPP), glutaraldehyde (GA), calcium chloride dihydrate, copper(II) sulfate, strontium chloride hexa-hydrate, sodium gluconate, D-glucose, Pluronic F127, and HEPES. Green-fluorescent latex nanospheres (nominal diameter of 100 nm) were obtained from Polysciences (catalog no. 17150). Carbon black particles (N110) were obtained from Sid Richardson Carbon Company.

Synthesis of Capsules and Beads. A pulsed-gas-flow micro-capillary device was used to prepare microscale capsules and beads. For the killer capsules, a 2 wt % chitosan solution in 0.2 M acetic acid with dispersed GOx was injected at 1.5 $\mu\text{L}/\text{min}$ through a silica capillary (diameter of 100 μm). Gas pulses (3 Hz; 9 psi) were applied at the orifice by a digital gas flow controller, as shown in Figure 2. The droplets were collected in an aqueous TPP solution (10 wt %) for 30 min and then incubated in GA (1 wt %) for 1 h. The capsules were then washed with DI water (five times) and were stored in DI water at 4 °C. For the target beads, the same above conditions were used with the difference being that the injected solution was 2 wt % sodium alginate in DI water, and the collection solution was 1 wt % CuSO_4 with 0.3 wt % Pluronic F127 added as a surfactant. The droplets were allowed to cross-link in the collection solution for 30 min. The final beads were then washed with DI water (five times) and were stored in DI water at 4 °C. For the inert beads, the injected solution was a mixture of 2 wt % chitosan in 0.5 M acetic acid with 1 wt % carbon black. Droplets were collected in 2 wt % GA and incubated for 24 h to form the inert chitosan–GA microbeads. All of the capsules and beads remain stable in solution for a period of several days. For the macroscale capsules and beads, instead of the above microfluidic device, millimeter-scale droplets were formed by extruding the appropriate solution through a 22 gauge needle. All other conditions were identical to those above.

Bead Degradation Experiments. For the experiments in Figure 3, the killer capsules and target beads were mixed at roughly equal ratios in a buffered solution (0.02 M HEPES; pH of 7.4) containing 1 wt % glucose. Bright-field microscopy images (10 \times objective) were taken every 5 min. For the experiments in Figure 5, the killer capsules, target beads, and inert beads were mixed at roughly equal ratios in the same solution as above, and the system was again monitored by bright-field microscopy.

Optical and Fluorescence Microscopy. A Zeiss Axiovert 135 TV inverted light microscope equipped with TouPView Imaging software was used for bright-field microscopy. Images were obtained with either a 2.5 \times or a 10 \times objective. For the studies on the release of fluorescent latex nanospheres (Figure S5), fluorescence images were taken using a band-pass excitation filter (530–585 nm) and a long pass emission filter of 615 nm.

ASSOCIATED CONTENT

Supporting Information

The Supporting Information is available free of charge on the ACS Publications website at DOI: 10.1021/acsami.6b10097.

Our analysis procedure for calculating percent degradation (Figure S1); Results on macroscale beads subjected to enzyme (Figure S2); Results on macroscale capsule-bead pairs (Figure S3); The effect of GOx enzyme concentration on degradation time (Figure S4); Results for the release of a fluorescent payload upon degradation of a target bead by a killer capsule (Figure S5). (PDF) A movie showing the bead degradation process in Figure 3 from start to finish. (MPG)

AUTHOR INFORMATION

Corresponding Author

*E-mail: sraghava@umd.edu.

Notes

The authors declare no competing financial interest.

ACKNOWLEDGMENTS

We acknowledge the contributions of three undergraduate students, Camila Saez, Hubert Huang, and Jacob Reinhart, to some of the experiments described in this paper.

REFERENCES

- (1) De Geest, B. G.; De Koker, S.; Sukhorukov, G. B.; Kreft, O.; Parak, W. J.; Skirtach, A. G.; Demeester, J.; De Smedt, S. C.; Hennink, W. E. Polyelectrolyte Microcapsules for Biomedical Applications. *Soft Matter* **2009**, *5*, 282–291.
- (2) Musyanovych, A.; Landfester, K. Polymer Micro- and Nano-capsules as Biological Carriers with Multifunctional Properties. *Macromol. Biosci.* **2014**, *14*, 458–477.
- (3) Andrade, B.; Song, Z. Y.; Li, J.; Zimmerman, S. C.; Cheng, J. J.; Moore, J. S.; Harris, K.; Katz, J. S. New Frontiers for Encapsulation in the Chemical Industry. *ACS Appl. Mater. Interfaces* **2015**, *7*, 6359–6368.
- (4) Esser-Kahn, A. P.; Odom, S. A.; Sottos, N. R.; White, S. R.; Moore, J. S. Triggered Release from Polymer Capsules. *Macromolecules* **2011**, *44*, 5539–5553.
- (5) Wang, H. C.; Zhang, Y. F.; Possanza, C. M.; Zimmerman, S. C.; Cheng, J. J.; Moore, J. S.; Harris, K.; Katz, J. S. Trigger Chemistries for Better Industrial Formulations. *ACS Appl. Mater. Interfaces* **2015**, *7*, 6369–6382.
- (6) He, Q.; Cui, Y.; Li, J. B. Molecular Assembly and Application of Biomimetic Microcapsules. *Chem. Soc. Rev.* **2009**, *38*, 2292–2303.
- (7) Stadler, B.; Price, A. D.; Chandrawati, R.; Hosta-Rigau, L.; Zelikin, A. N.; Caruso, F. Polymer Hydrogel Capsules: En Route Toward Synthetic Cellular Systems. *Nanoscale* **2009**, *1*, 68–73.
- (8) Gupta, A.; Terrell, J. L.; Fernandes, R.; Dowling, M. B.; Payne, G. F.; Raghavan, S. R.; Bentley, W. E. Encapsulated Fusion Protein Confers “Sense And Respond” Activity to Chitosan-Alginate Capsules to Manipulate Bacterial Quorum Sensing. *Biotechnol. Bioeng.* **2013**, *110*, 552–562.
- (9) Alberts, B. *Mol. Biol. Cell*, 4th ed.; Garland Publishers: New York, 2002.

- (10) Paul, W. E. *Fundamental Immunology*, 7th ed.; Garland Publishers: New York, 2013.
- (11) Tschopp, J.; Nabholz, M. Perforin-Mediated Target-Cell Lysis by Cytolytic Lymphocyte-T. *Annu. Rev. Immunol.* **1990**, *8*, 279–302.
- (12) Vollenweider, I.; Groscurth, P. Ultrastructure of Cell-Mediated Cytotoxicity. *Electron Microsc. Rev.* **1991**, *4*, 249–267.
- (13) Lu, A. X. “Microfluidic Generation of Anisotropic Capsules.” Ph.D. Dissertation, University of Maryland, 2015.
- (14) Ghaffarian, R.; Perez-Herrero, E.; Oh, H.; Raghavan, S. R.; Muro, S. Chitosan-Alginate Microcapsules Provide Gastric Protection and Intestinal Release of ICAM-1-Targeting Nanocarriers, Enabling GI Targeting In Vivo. *Adv. Funct. Mater.* **2016**, *26*, 3382–3393.
- (15) Kontturi, L. S.; Yliperttula, M.; Toivanen, P.; Maatta, A.; Maatta, A. M.; Urtti, A. A Laboratory-Scale Device for the Straightforward Production of Uniform, Small Sized Cell Microcapsules with Long-Term Cell Viability. *J. Controlled Release* **2011**, *152*, 376–381.
- (16) Jiang, K. Q.; Lu, A. X.; Dimitrakopoulos, P.; Devoe, D. L.; Raghavan, S. R. Microfluidic Generation of Uniform Water Droplets Using Gas as the Continuous Phase. *J. Colloid Interface Sci.* **2015**, *448*, 275–279.
- (17) Peniche, C.; Arguelles-Monal, W.; Peniche, H.; Acosta, N. Chitosan: An Attractive Biocompatible Polymer for Microencapsulation. *Macromol. Biosci.* **2003**, *3*, 511–520.
- (18) Ohkawa, K.; Kitagawa, T.; Yamamoto, H. Preparation and Characterization of Chitosan-Gellan Hybrid Capsules Formed by Self-Assembly at an Aqueous Solution Interface. *Macromol. Mater. Eng.* **2004**, *289*, 33–40.
- (19) Lee, H. Y.; Tiwari, K. R.; Raghavan, S. R. Biopolymer Capsules Bearing Polydiacetylenic Vesicles as Colorimetric Sensors of pH and Temperature. *Soft Matter* **2011**, *7*, 3273–3276.
- (20) Arya, C.; Kralj, J. G.; Jiang, K. Q.; Munson, M. S.; Forbes, T. P.; DeVoe, D. L.; Raghavan, S. R.; Forry, S. P. Capturing Rare Cells From Blood Using a Packed Bed of Custom-Synthesized Chitosan Microparticles. *J. Mater. Chem. B* **2013**, *1*, 4313–4319.
- (21) Huang, Y.; Lapitsky, Y. Salt-Assisted Mechanistic Analysis of Chitosan/Tripolyphosphate Micro- and Nanogel Formation. *Biomacromolecules* **2012**, *13*, 3868–3876.
- (22) Ghanem, A.; Ghaly, A. Immobilization of Glucose Oxidase in Chitosan Gel Beads. *J. Appl. Polym. Sci.* **2004**, *91*, 861–866.
- (23) Barakat, N. S.; Almurshedi, A. S. Preparation and Characterization of Chitosan Microparticles for Oral Sustained Delivery of Gliclazide: In Vitro/In Vivo Evaluation. *Drug Dev. Res.* **2011**, *72*, 235–246.
- (24) Dowling, M. B.; Bagal, A. S.; Raghavan, S. R. Self-Destructing “Mothership” Capsules for Timed Release of Encapsulated Contents. *Langmuir* **2013**, *29*, 7993–7998.
- (25) Ouwerx, C.; Velings, N.; Mestdagh, M. M.; Axelos, M. A. V. Physico-Chemical Properties and Rheology of Alginate Gel Beads Formed with Various Divalent Cations. *Polym. Gels Networks* **1998**, *6*, 393–408.
- (26) Fundueanu, G.; Nastruzzi, C.; Carpov, A.; Desbrieres, J.; Rinaudo, M. Physico-Chemical Characterization of Ca-Alginate Microparticles Produced with Different Methods. *Biomaterials* **1999**, *20*, 1427–1435.
- (27) Morch, Y. A.; Donati, I.; Strand, B. L.; Skjak-Braek, G. Effect of Ca²⁺, Ba²⁺, and Sr²⁺ on Alginate Microbeads. *Biomacromolecules* **2006**, *7*, 1471–1480.
- (28) Liu, Y.; Javvaji, V.; Raghavan, S. R.; Bentley, W. E.; Payne, G. F. Glucose Oxidase-Mediated Gelation: A Simple Test To Detect Glucose in Food Products. *J. Agric. Food Chem.* **2012**, *60*, 8963–8967.
- (29) Peters, R. W. Chelant Extraction of Heavy Metals from Contaminated Soils. *J. Hazard. Mater.* **1999**, *66*, 151–210.
- (30) Smith, R. A.; Martell, A. E. NIST Critically Selected Stability Constants of Metal Complexes Database: Version 8.0. NIST Standard Reference Database 46; NIST: Gaithersburg, MD, 1997.
- (31) Good, N. E.; Izawa, S. Hydrogen Ion Buffers. *Methods Enzymol.* **1972**, *24*, 53–68.
- (32) Bird, R. B.; Stewart, W. E.; Lightfoot, E. N. *Transport Phenomena*, 2nd ed.; Wiley: New York, 2002.

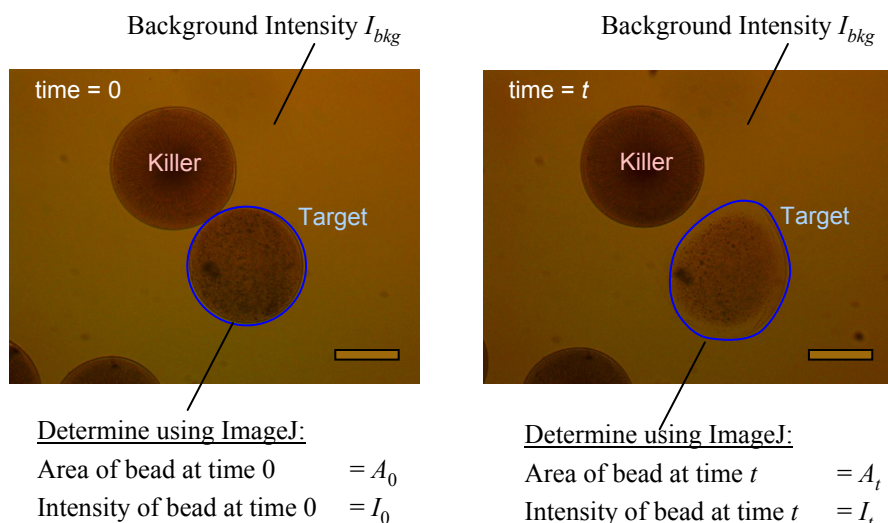
Supporting Information for:

“Killer” Microcapsules That Can Selectively Destroy Target Microparticles in Their Vicinity

Chandamany Arya, Hyuntaek Oh and Srinivasa R. Raghavan*

Department of Chemical and Biomolecular Engineering, University of Maryland, College Park, MD 20742-2111

*Corresponding author. Email: sraghava@umd.edu



$$\% \text{ Undegraded} = (\text{Normalized Opacity}) \cdot (\text{Normalized Area})$$

$$= \left(\frac{I_t - I_{bkg}}{I_0 - I_{bkg}} \right) \cdot \left(\frac{A_t}{A_0} \right)$$

Figure S1. Procedure for calculating the % of the target bead that is undegraded at a given time t . The analysis is done using the Image J program. The contour of the target bead is traced, as shown in blue, and then the area within this trace and the intensity (total pixels within this area) are determined by the program.

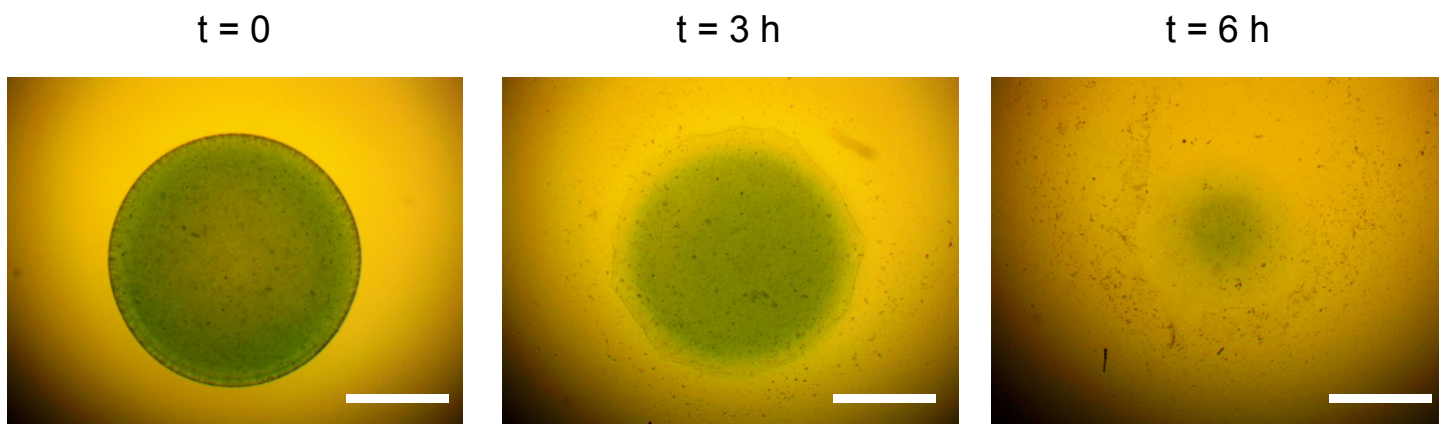


Figure S2. Degradation of target Cu-alginate beads by addition of GOx enzyme to the solution. The bead is placed in a solution containing 1 wt% glucose and 1 unit/mL of GOx is added. The optical microscopy images over time show that the bead degrades over the course of 6 h. When the same experiment is conducted without glucose or without the GOx, no degradation is observed. Scale bars represent 1 mm.

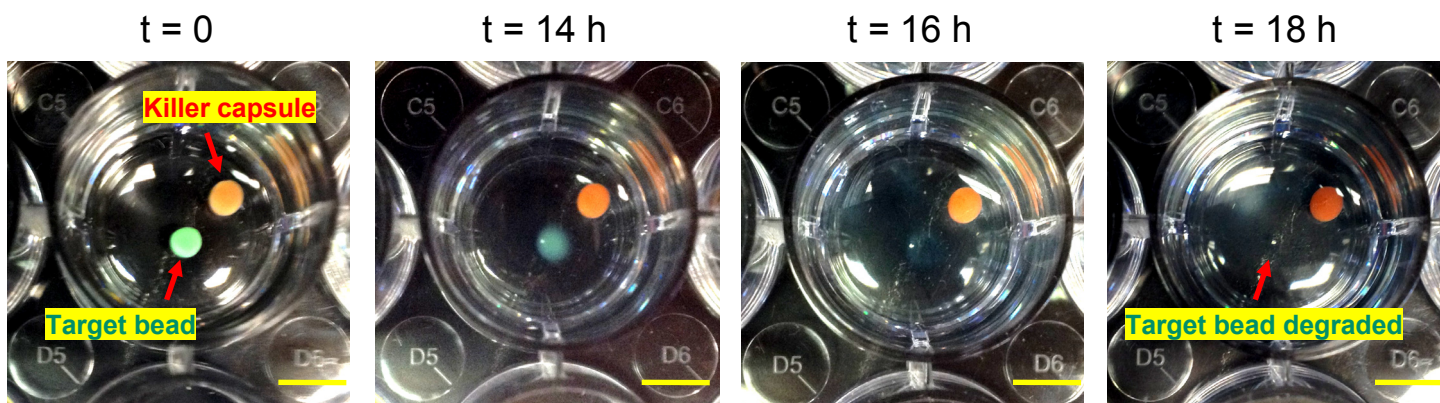


Figure S3. Degradation of macroscale target beads by corresponding killer capsules. At $t = 0$, a killer capsule and target bead (each of diameter ~ 2.5 mm) are placed close to each other in a HEPES buffer solution containing 1 wt% of glucose. The killer is a chitosan-TPP-GA capsule with 200 units/mL of GOx inside it. The target is alginate cross-linked with 1 wt% CuSO_4 . The photographs over time show that in 18 h, the target bead is completely degraded. Scale bars represent 5 mm.

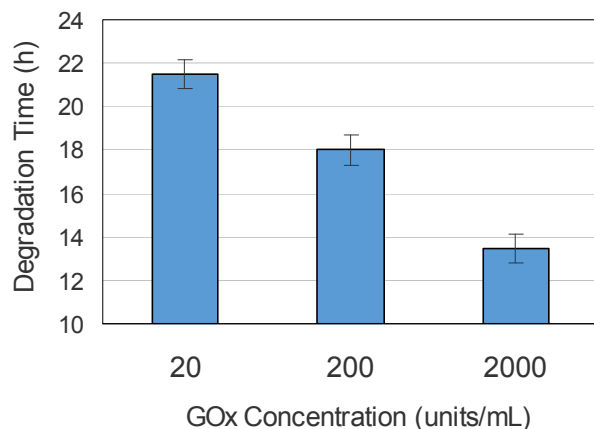


Figure S4. Effect of GOx enzyme concentration on degradation time. The experiment in Figure S3 was repeated with other concentrations of GOx in the killer capsule. The degradation time is defined as the time it takes to completely degrade the target bead, and the data show that this time decreases monotonically with increasing GOx concentration. The error bars correspond to the standard deviation from three measurements.

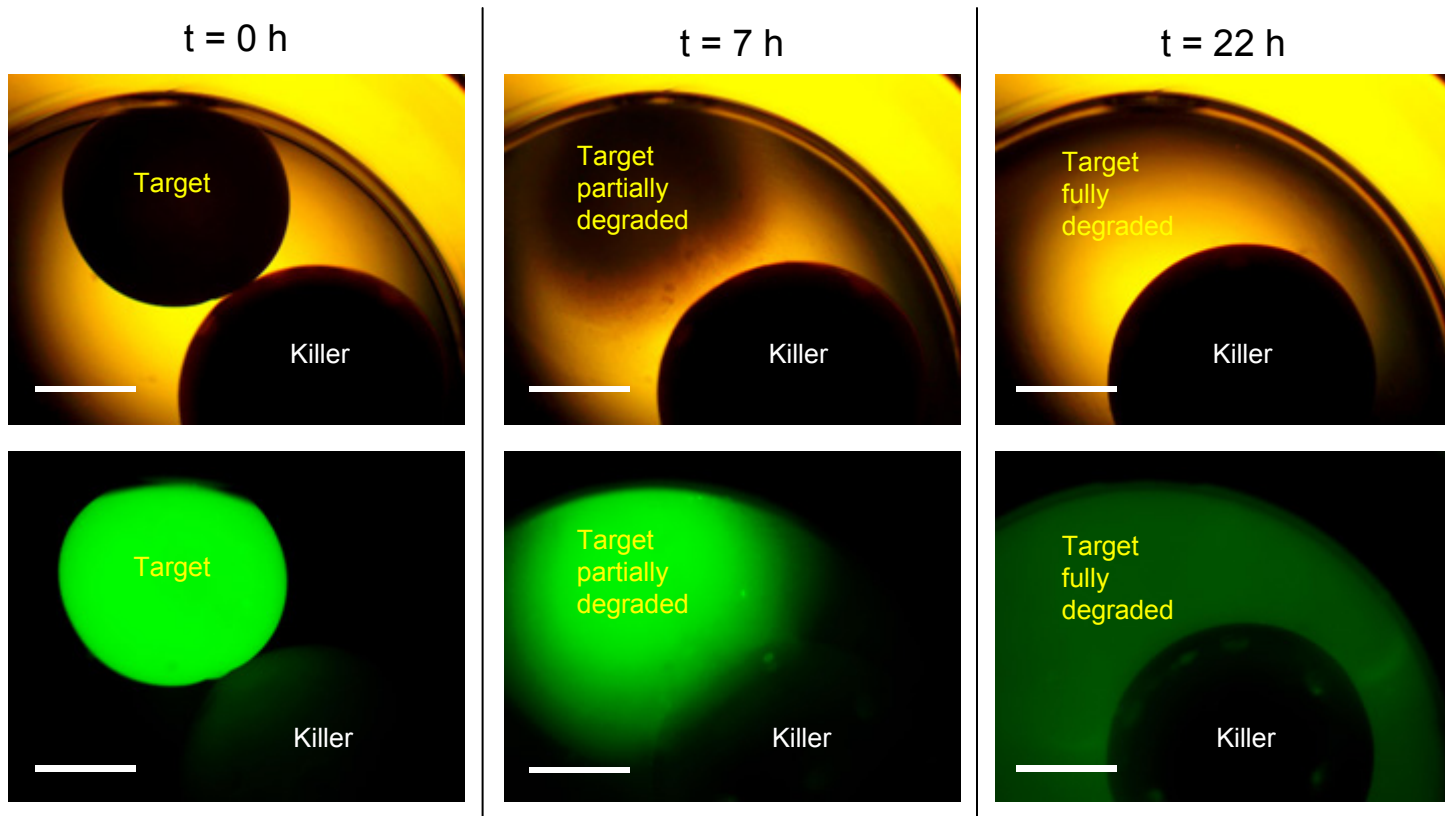


Figure S5. Release of fluorescent payload upon degradation of a target bead by a killer capsule. At $t = 0$, a killer chitosan/GOx capsule (200 units/mL of GOx) and a target Cu-alginate bead containing green-fluorescent nanoparticles (diameter of ~ 100 nm) are placed next to each other in a HEPES buffer solution containing 1 wt% of glucose. Optical microscopy images under brightfield (top row) and fluorescence (bottom row) are shown at various time points. Initially, the fluorescence is contained within the target bead. At the 7h mark, there is partial degradation of the target, and as a result, the fluorescent nanoparticles are released out of the bead. Thus, the fluorescence is spread over a larger area. At the 22 h mark, the degradation is complete and the target can no longer be detected in the brightfield image. By this time, the nanoparticles have diffused throughout the solution, which thereby shows a uniform green fluorescence. The scale bars represent 1 mm.